

Prewetting of Liquid Hydrogen on Rough Cesium Substrates

E. Rolley and C. Guthmann

*Laboratoire de Physique Statistique de l'ENS, 24 rue Lhomond, 75005 Paris, France,
Associé au CNRS et aux Universités Paris 6 et Paris 7, France*

M. S. Pettersen

*Washington and Jefferson College, 60 S. Lincoln Street, Washington, Pennsylvania 15301, USA
(Received 13 January 2009; published 2 July 2009)*

We have studied the prewetting dynamics of H_2 on rough Cs substrates obtained by low temperature deposition. The boundary between the thin and the thick van der Waals film is strongly pinned and distorted by the defects of the substrate. Comparing prewetting and wetting dynamics allows us to show that the dynamics and the geometry of the thin-thick boundary cannot be accounted for in a simple 1D model. The finite width of the boundary makes its behavior similar in many aspects to the one of a contact line.

DOI: 10.1103/PhysRevLett.103.016101

PACS numbers: 68.08.Bc, 68.03.Fg, 68.15.+e

For a system of two fluid phases at equilibrium, the wetting transition on a surface is usually first order [1]. In this case, the wetting transition extends off coexistence to what is called the prewetting transition [1,2]. In the simple case of a liquid-vapor phase equilibrium in the presence of a surface, the coverage changes at the prewetting transition from a thin film to a thick but finite film, which correspond to the wetted state at coexistence.

In principle, the transition between a thin and a thick film state occurs at a prewetting line in the $T - \Delta\mu$ plane. However, many experiments have shown that the transition is hysteretic [3–5]. As for any first order transition, this hysteresis could be due to a nucleation energy barrier [1]. In the case of solid substrate, another origin for this hysteresis can be the pinning of the edge of the thick film on defects of the substrate [6,7]. The first direct evidence for this mechanism has been provided by Dupont-Roc and co-workers for the helium or cesium system [8]. Yet, experimental data on the dynamics of the film edge are very limited.

A better understanding of the film edge dynamics would be useful for the interpretation of the existing data on the prewetting transition of cryogenic fluids on alkali. More generally, the film edge on a disordered substrate is an example of an elastic line in a random potential energy landscape, a problem to which much theoretical work has been devoted in the last decade (see [9,10] and ref. therein). The dynamics of the film edge off coexistence is closely related to the dynamics of the meniscus edge—or contact line—at coexistence: in both cases, the hysteresis is due to the pinning of an elastic line by the substrate heterogeneities. However, one expects the elastic restoring force to be very different: a film edge is a true line characterized by a line tension while the contact line stiffness stems from the liquid-vapor surface tension, which leads to nonlocal elasticity [11].

In this Letter, we demonstrate that using liquid H_2 allows us to study both the film edge and the contact line on the same disordered substrate. The difference in elasticity makes the geometry of the boundary quite different for the two systems, although the structure of the film edge makes this difference more subtle than previously thought.

Experimental system and setup.—The wetting transition of H_2 on Cs is well documented [12,13]. H_2 was chosen rather than Helium-4 because its optical index ($n - 1 \approx 0.12$) is higher than that of He ($n - 1 \approx 0.026$). Thus, the film edge can be imaged directly, and the film thickness can be measured without using complex methods such as surface plasmon resonance [14], Nomarski microscopy [15], or ellipsometry [16]. Cesium is deposited at low temperature as described in Ref. [17] (100 Cs atomic layers annealed at 150 K), which yields rough substrates with a lateral length scale of roughness of the order of 10 nm [17–19].

Cs is deposited on a silicon wafer which can be dipped into or out of the H_2 bath [17]. The Cs-plated wafer is illuminated at normal incidence by a monochromatic source (633 nm). An image of the receding meniscus at 18 K is shown in Fig. 1. The contact angle θ is inferred from the measurement of the capillary rise h with respect to the asymptotic level of the H_2 bath. Varying the plate velocity allows us to obtain θ as a function of the velocity V of the contact line with respect to the substrate [17]. The wetting hysteresis H_{cl} is then defined as: $H_{cl} \equiv \gamma(\cos\theta_{r0} - \cos\theta_{a0})$, where γ is the liquid-vapor surface tension and θ_{a0} (resp. θ_{r0}) is the advancing (resp. receding) contact angle measured at a small velocity chosen arbitrarily to be 3 $\mu\text{m/s}$. As in previous experiments, H_{cl} is about 0.1 γ .

When the receding contact angle θ_{r0} is smaller than 10° ($T \approx 18$ K), a film is left on the plate when it is pulled out of the bath. The film thins within a few minutes due to both evaporation and draining until it reaches a state where the

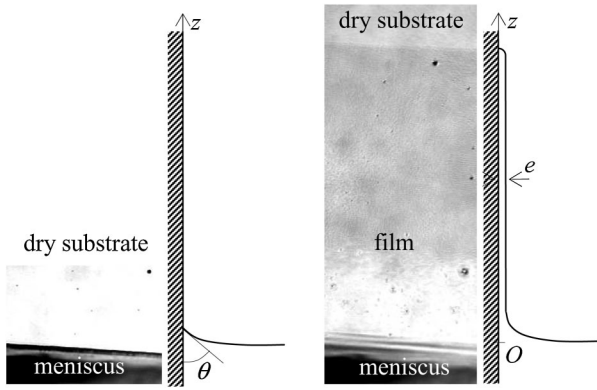


FIG. 1. The plate has been dipped in and out of the bath. Left: $T = 18.000$ K. The meniscus recedes with a finite contact angle θ_r . Right: $T = 18.103$ K. A metastable film remains. (image width: 2 mm).

thickness e is constant. As shown in Fig. 1, this thick film appears slightly darker than the “dry” substrate which is actually covered by a submonolayer thin film. The contrast is due to the interference between the light reflected at the liquid-vapor interface and the light reflected at the liquid-Cs interface. Knowing the optical index of H_2 [20], e can be measured from the contrast. We find $e = 50 \pm 20$ nm. We cannot detect any variation of e as a function of the height z with respect to the liquid bath level, at least for z in the range 2–10 mm. Furthermore, e does not depend on the temperature in the range 18–20 K.

For H_2 on Cs, the equilibrium film thickness is set by the competition between gravity and van der Waals forces: $e = (\Delta C_3/mgz)^{1/3}$, with $\Delta C_3 \equiv C_3^{Cs} - C_3^{H_2}$, m the mass of a H_2 molecule, and g the gravitational acceleration. The C_3 's are the coefficients of the van der Waals potentials between an H_2 molecule and a semi-infinite slab of Cs or bulk H_2 . With $\Delta C_3 = 2400 \text{ K} \cdot \text{\AA}^3$ [12,21] and $z = 5$ mm, one finds $e = 59$ nm in agreement with the experimental value. The fact that we do not observe the $z^{-1/3}$ dependence could be due to the limited range in z and to the poor accuracy on e . Correcting vdW potential for retardation effects, as proposed by Cheng and Cole [22], leads to $e = 49$ nm for $z = 5$ mm in even better agreement with the measured value.

Behavior of the contact line.—We first measured the dynamics of the contact line (CL), that is, the dependence of the velocity V as a function of the applied force f_{CL} which is here the unbalanced Young force: $f_{CL} = \gamma(\cos\theta - \cos\theta_{eq})$ where θ_{eq} is the equilibrium contact angle [17]. As in previous experiments [17], V varies exponentially with f_{CL} . Assuming that the dynamics is thermally activated, we have fitted the advancing and receding branches by simple Arrhenius laws characterized by activation lengths λ_a and λ_r and activation energies E_a^* and E_r^* . We find that the activation lengths are about 20 nm, and that the typical activation energy $\epsilon^* \equiv E_a^*/\lambda_a^2 + E_r^*/\lambda_r^2$ is of the order of the hysteresis H_{CL} . The numerical

values (Table I) are close to the ones previously published and show that the size of activated jumps is of order of the topological defects of the substrate. This is a situation of *strong* pinning in the sense that individual defects are strong enough to pin the CL.

As seen in Fig. 1, the disorder does not cause any visible distortion of the CL. The amplitude w of the CL fluctuations is expected to scale with the length L of the CL as $w/\xi \sim (L/\xi)^{0.5}$, where ξ is the correlation length of the disorder [9]. With $\xi \approx 20$ nm and $L \approx 2$ mm, one finds $w \approx 6 \mu\text{m}$, of the order of the optical resolution.

Behavior of the edge of the vdW film.—The thin and the thick films are in equilibrium on the prewetting line, where the spreading coefficient $S(\Delta\mu, T) = 0$. Most observations are done for a film edge at roughly $z = 5$ mm above bulk liquid level, that is, at a fixed departure from liquid-vapor equilibrium $\Delta\mu = mgz$. Thus, one controls S , and hence the departure from the prewetting line, mainly by changing the temperature. An experimental run consists in coating half of the plate by a thick film and monitoring the film edge (FE) at constant or slowly varying T .

We find that the film edge does not move for $18 \leq T \leq 20$ K. When the temperature is lower than about 18 K, the substrate dries through the receding of the FE. The receding edge is strongly distorted and moves discontinuously through successive jumps; a sequence is shown in Fig. 2. The FE displays overhangs; islands can also be observed, but they evaporate soon after they become disconnected from the main film. Note that dewetting occurs first at the right edge of the plate rather than at the top, as one may have expected. We think that the Cs deposition and annealing is not quite uniform, which causes large-scale variations of the spreading coefficient S . These variations are more important than the effect of gravity and may partly explain why no z dependence of the film thickness is observed. As the shape of the FE is qualitatively the same for the edge receding downwards or upwards [early stage in Fig. 2], draining is presumably not relevant, and the liquid removal is mainly due to evaporation.

The distortions of the edge are orders of magnitude larger than that of the CL. The distortions result from the balance between the pinning forces and the elastic restoring force of the boundary. In both situations, the disorder arises from the substrate roughness. To first approximation, the local slope of the substrate is equivalent to a local change in the spreading coefficient S around the mean value \bar{S} [11]. If the hillocks of the Cs surface are small crystals, then the different sides of the hillocks have differ-

TABLE I. Wetting properties of the Cesium substrate.

T (K)	θ_{a0} (degrees)	θ_{r0} (degrees)	H_{cl}/γ	λ_a (nm)	λ_r (nm)	ϵ^*/γ
15	45 ± 2	32.5 ± 2	0.135	20	18	0.071
18	29.5 ± 2	8 ± 2	0.120	19	18	0.065
20	8 ± 2	0

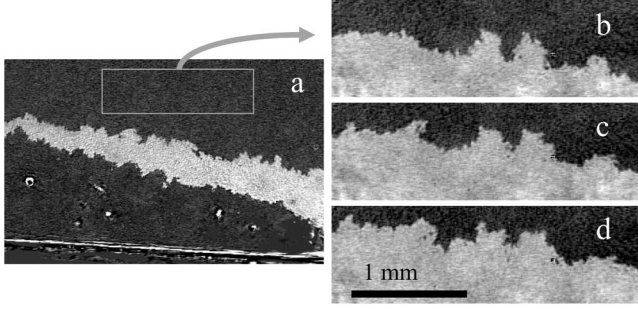


FIG. 2. Successive images of the receding film at $T = 18.155$ K. (a) early stage: dewetting occurs at the right of the plate and the dry (bright) area extends first towards the center. (b), (c), (d) Enlarged images of the rectangle in (a) at later times: the dry area widens (time interval: 500 s).

ent crystalline orientation and hence different S [23]. Whatever the exact mechanism, the amplitude of the disorder is similar in both cases and can be characterized by ΔS defined by $(\Delta^2 S = \overline{(S - \bar{S})^2})$. Thus, the main difference between the two boundaries arises from the difference in the elastic restoring force: it is long-ranged for the CL while it is short-ranged for the FE characterized by a line tension τ , or energy per unit length.

The prewetting situation has been mapped into a Random Field Ising Model (RFIM): the local thin or thick films represent the two spin states, the random part $S(\vec{r}) - \bar{S}$ of the spreading coefficient acts as a random field, and the line tension is associated with the ferromagnetic coupling [7]. For RFIM, one expects that the domains are compact on a scale smaller than the persistence length l_c (elastic forces win at small scale), and that the boundary is more fractal at larger length scale (disorder wins at large scale). More precisely, one expects that $l_c/\lambda \sim \exp(\tau/\lambda\Delta S)^2$. For our system, l_c can be roughly estimated from the typical width of the fingers of the film edge, yielding l_c of the order of $10 \mu\text{m}$ as found in Ref. [8]. Here, we cannot analyze more accurately the shape of the FE because the thick film domain is compact at large scale. We think that this is due to the large scale variation of \bar{S} which acts as a stabilizing external field gradient and kills the large fluctuations of the boundary. Whatever the exact value of l_c , the important point is that it is much larger than the disorder length scale λ : the disorder is weak (or $\lambda\Delta S < \tau$).

When the temperature is increased from 20 up to 20.3 K, the dry part of the substrate is progressively covered by the thick film. However, no motion of the FE is detected: the liquid coverage increases continuously with T from almost zero up to 50 nm. A similar behavior has been observed for the He/Cs system with strongly disordered Cs substrate [24]. As any coverage intermediate between the thin and the thick vdW film is unstable, it is likely that the thick film is actually lacunary at a length scale smaller than the optical resolution (here $5 \mu\text{m}$). The increase of the mean coverage could be due to the condensation of small drop-

lets or the advancing of “fingers” whose width is smaller than the resolution. This is surprising in view of Fig. 2, where the thick film domain is very compact. The asymmetry between advancing and receding is also surprising in view of a previous experiment on the He/Cs system where the receding and advancing front displayed similar geometries [8].

Dynamics of the edge of the vdW film.—As stressed above, the motion of the film edge can only be detected in the drying case. We monitor the receding FE at constant T . The velocity V of the film edge is defined as $V = \dot{A}/L$ where \dot{A} is the area swept per unit time by a line of length $L \simeq 5$ mm. To avoid the effects of large-scale heterogeneities, V is measured on the same region of the substrate in all runs. This also ensures that $\Delta\mu = mgz$ is constant. As shown in Fig. 3, we find that V varies strongly with the temperature around 18 K: it increases by 3 orders of magnitude when T decreases by less than 0.1 K.

The relevant parameter is the force acting on the FE rather than T . In the case of the FE, the force per unit length f_{fe} is the mean value of $S(T, \Delta\mu)$. As the FE is pinned in a large temperature range, we cannot determine the true equilibrium temperature so that the applied force is known only within a constant.

Off liquid-vapor coexistence, $S(T, \Delta\mu) = \gamma_{\text{SV}} - \gamma_{\text{SL}} - \gamma - \delta S_{\text{film}}$, where γ_{SV} and γ_{SL} are the surface tensions of the solid-vapor and solid-liquid interfaces and δS_{film} is the film contribution. $\delta S_{\text{film}} = (3/2)\Delta C_3(\rho_L - \rho_V)\Delta\mu^{2/3}$ where ρ_L and ρ_V are the liquid and vapor densities.

Here, $\Delta\mu$ is sufficiently small such that δS_{film} is negligible compared to the temperature variation of $S(T, 0) = \gamma_{\text{SV}} - \gamma_{\text{SL}} - \gamma = \gamma(\cos\theta_{\text{eq}} - 1)$. With the usual assumption $\theta_a \simeq \theta_{\text{eq}}$ [12,13], one finds that S varies roughly linearly with T . Then the relation between the applied force and T is simply: $df_{\text{fe}}/dT \simeq 0.13 \text{ mN} \cdot \text{m}^{-1} \text{ K}^{-1}$ [25].

Thus, the 2 K hysteresis in T corresponds to a hysteresis in force $H_{\text{fe}} \simeq 0.26 \text{ mN/m}$ or $H_{\text{fe}} \simeq H_{\text{cl}}$. For the receding edge, the shape of $V(S)$ is the same as the one of $V(T)$. From the semilog plot of Fig. 3, it can be seen that V varies roughly like $\exp|S|$. The simplest interpretation is that the motion of the film edge obeys an Arrhenius’

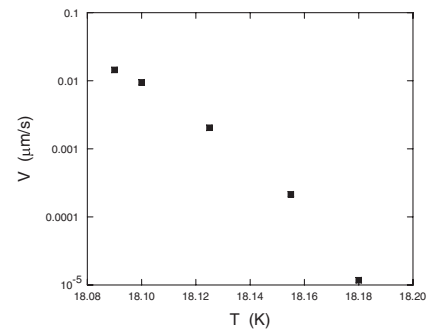


FIG. 3. Mean velocity of the film edge as a function of the temperature.

law: $V \propto \exp(\frac{\lambda_{fe}^2 |S|}{2k_B T})$. One finds that the activation length λ_{fe} is about 17 nm, very close to the values of the activation lengths obtained for the CL. This strongly supports the idea that the same disorder is responsible for the pinning of both the film edge and the contact line, and that the dynamics of both boundaries are controlled by thermal depinning at the scale of a *single* defect.

This simple interpretation is contradictory with a previous analysis of experiments on He/Cs systems [8,26] which have been analyzed in term of creep motion, in close analogy with the dynamics of magnetic systems [27]. In that case, V scales like $\exp[(S_C/S)^\mu]$ because energy barriers for depinning diverge for vanishing driving force S . Hence, a true creep regime can only be observed for forces S small compared to the depinning threshold S_C . This is *not* the case in the He/Cs system. We think that experimental data are consistent with our interpretation: Fig. 3 in Ref. [8] exhibits the same exponential behavior as we observed.

A closer look at Fig. 3 shows that $\log V$ varies more slowly than $|S|$, so one may wonder whether a more accurate fit of the data can be obtained by going beyond a simple Arrhenius law. Taking into account the distribution of pinning defects leads to an algebraic temperature dependence in the prefactor of the exponential [28], but the temperature range here is too small for such an effect to be important. Rather, we think that the FE motion is limited by the removing of the liquid. At high velocity ($V > 1 \mu\text{m/s}$), a rim is visible at the film edge indicating that evaporation is not fast enough to remove the liquid.

Discussion.—Even if we cannot account quantitatively for the departure from a true exponential behavior, it is very likely that the dynamics of the FE is thermally activated and that the size of the elementary depinning events is in the 10 nm range. As in the case of the CL, this corresponds to a *strong* pinning situation. This is contradictory with the large value of the persistence length which seems to correspond to a *weak* pinning situation.

We propose the following explanation: the RFIM approach is not relevant at small length scales because the FE is not a true 1D system. For a vdW film of thickness e , the lateral extension of a disturbance in the film thickness, or “healing” length Λ is given by the balance between surface tension and vdW forces: $\Lambda \simeq [\gamma/(v\Delta C_3)]^{1/2} e^2$, where v is the molecular volume [29]. One expects that the width of the FE is of order Λ . For H_2/Cs , one finds $\Lambda \simeq 3 \mu\text{m}$, much larger than the size λ of the defects. Only for length scales larger than Λ can the FE be considered as a true line, in which case the RFIM description is valid. So the persistence length is set by the structure of the FE rather than by the balance between elastic and pinning forces. For length scales smaller than Λ , the film edge is similar to a meniscus. This is consistent with defects pinning both the CL and the film edge in the same way.

We still have to explain the behavior of the advancing film. We have argued that advancing is likely to occur in qualitatively the same way as the receding, but with a

persistence length notably smaller. At the moment, we have no precise picture of the shape and behavior of the film edge between or above the hillocks of the substrate at the nm scale. We still have to understand how this behavior is changed between 18 and 20 K. Further experiments at various desaturation $\Delta\mu$ would be helpful as changing $\Delta\mu$ allows us to vary two key parameters, the healing length and the line tension, at constant temperature.

-
- [1] D. Ross and D. Bonn, Rep. Prog. Phys. **64**, 1085 (2001).
 - [2] C. Ebner and W. Saam, Phys. Rev. B **35**, 1822 (1987).
 - [3] J.E. Rutledge and P. Taborek, Phys. Rev. Lett. **69**, 937 (1992).
 - [4] K. S. Ketola, S. Wang, and R. B. Hallock, Phys. Rev. Lett. **68**, 201 (1992).
 - [5] H. Kellay, D. Bonn, and J. Meunier, Phys. Rev. Lett. **71**, 2607 (1993).
 - [6] C. S. Nolle *et al.*, Physica A (Amsterdam) **205**, 342 (1994).
 - [7] R. Blosssey, T. Kinoshita, and J. Dupont-Roc, Physica A (Amsterdam) **248**, 247 (1998).
 - [8] X. Müller and J. Dupont-Roc, Europhys. Lett. **54**, 533 (2001).
 - [9] S. Moulinet, C. Guthmann, and E. Rolley, Eur. Phys. J. E **8**, 437 (2002).
 - [10] S. Moulinet, C. Guthmann, and E. Rolley, Eur. Phys. J. B **37**, 127 (2004).
 - [11] P. G. De Gennes, Rev. Mod. Phys. **57**, 827 (1985).
 - [12] D. Ross, P. Taborek, and J. E. Rutledge, Phys. Rev. B **58**, R4274 (1998).
 - [13] M. S. Pettersen, E. Rolley, C. Guthmann, and M. Poujade, J. Low Temp. Phys. **134**, 281 (2004).
 - [14] S. Herminhaus *et al.*, Ann. Phys. (N.Y.) **6**, 425 (1997).
 - [15] X. Müller, T. Kinoshita, and J. Dupont-Roc, Rev. Sci. Instrum. **72**, 2069 (2001).
 - [16] T. McMillan, J. E. Rutledge, and P. Taborek, J. Low Temp. Phys. **138**, 995 (2005).
 - [17] E. Rolley and C. Guthmann, Phys. Rev. Lett. **98**, 166105 (2007).
 - [18] M. Zech *et al.*, J. Low Temp. Phys. **137**, 179 (2004).
 - [19] A. Fubel *et al.*, Surf. Sci. **601**, 1684 (2007).
 - [20] D. E. Diller, J. Chem. Phys. **49**, 3096 (1968).
 - [21] A. Chizmeshya, M. W. Cole, and E. Zaremba, J. Low Temp. Phys. **110**, 677 (1998).
 - [22] E. Cheng and M. W. Cole Phys. Rev. B **38**, 987 (1988).
 - [23] M. W. Cole, M. R. Swift, and F. Toigo, Phys. Rev. Lett. **69**, 2682 (1992).
 - [24] J. Dupont-Roc and X. Müller, Physica B (Amsterdam) **284–288**, 143 (2000).
 - [25] The symmetry between advancing and receding branches of $V(f)$ for the CL rather suggest $\cos\theta_{eq} = 1/2(\cos\theta_a + \cos\theta_r)$; this leads also to $dS/dT \simeq 0.13 \text{ mN} \cdot \text{m}^{-1} \text{ K}^{-1}$.
 - [26] J. Dupont-Roc, J. Low Temp. Phys. **126**, 339 (2002).
 - [27] S. Lemerle *et al.*, Phys. Rev. Lett. **80**, 849 (1998).
 - [28] D. Vandembroucq, R. Skoe, and S. Roux, Phys. Rev. E **70**, 051101 (2004).
 - [29] D. Andelman, J.-F. Joanny, and M. O. Robbins, Europhys. Lett. **7**, 731 (1988).